Numerical Analysis of Feedback System for Magnetic Levitation

Christopher Aceto
Physics Department
Lawrence University
Appleton, WI, USA
(A Positron-Electron eXperiment, Max-Planck-Institut für Plasmaphysik)
(Dated: November 26, 2020)

The APEX collaboration aims to create and study magnetized electron-positron pair plasmas. The plasma will be contained within the magnetic field of a levitated magnetic dipole. A coil of superconducting material, charged with a current via induction, creates the dipole field. The levitation of the dipole is naturally unstable, so an analog control system is implemented to provide stability. In this paper, I describe a time-domain model of the control system, as well as the results of numerical simulations of the model. Optimal settings for the control system are found, and the system is tested in various situations.

I. INTRODUCTION

Most plasmas that have been studied consist of oppositely charged particles with very different masses. It is relatively easy to create and study a plasma composed of negatively charged electrons and positively charged ions. Plasmas composed of equally massive charged particles (pair plasmas) have not been studied as extensively. This is due to the fact that it is very difficult to obtain the right particles to make such a plasma. For example, with pair plasmas composed of oppositely charged particle-antiparticle pairs, it is difficult to create and store a large quantity of antiparticles. Recently, though, the technology needed to accomplish this for positrons has made advances, and it is now becoming possible to create and study an electron-positron pair plasma.

In addition to obvious applications to antimatter physics, studying electron-positron pair plasma has important astrophysical applications. Many high-energy, radiating bodies, such as pulsars, neutron stars, and active galactic nuclei, can create pair plasmas as their gamma radiation interacts with surrounding matter. In fact, the relativistic jets created by some of these objects have been observed to be composed mainly of pair plasmas. Research on pair plasma will further understanding of these astronomical phenomena.

Electron-positron pair plasmas have some different properties from conventional plasmas that make them interesting. The particles in an electron-positron plasma all have very low mass, which means they accelerate much more in a magnetic field compared to heavier particles. This allows for studying magnetized plasma much more easily than with a heavier plasma.

Furthermore, density fluctuations and electric potential fluctuations are unrelated in an electron-positron pair plasma. In conventional plasmas, if there is a region of high density, the tiny electrons will escape the region quickly, while the heavy positive ions will remain. This creates a corresponding region of concentrated positive charge; hence, the electric potential fluctuates as the density fluctuates. This potential difference can create an acoustic wave that moves through the plasma. On the other hand, in an electron-positron pair plasma, the equally massive particles move away from a region of high density at the same rate, so no electric potential fluctuation is created.

This absence of correlation between density and electric potential has important implications. When conventional plasmas are magnetically trapped, there are instabilities created by the density-potential correlation (called the universal instability). The acoustic waves that this correlation creates grow in amplitude as they move through the plasma. However, since those waves should be absent from an electron-positron plasma, it is predicted that the universal instability would be absent from such a plasma. This stability, or suppression of turbulence, opens a lot of opportunity for experimentation. The above information about plasma is from Ref. [1].

The APEX collaboration at the Max Planck Institute for Plasma Physics plans to study electron-positron plasmas. Both a positron source (PAX) and a magnetic trap for the plasma (APEX) are in development. The trap will consist of a levitating, superconducting coil that serves as a magnetic dipole. The dipole must levitate because a mechanical support would distort the dipole magnetic field, and particles in the plasma would collide with the support. A superconducting coil can have a current induced, and then it can approximately conserve that current for a long duration.

A magnetic dipole is desired for the particle trap because it helps stabilize an electron-positron plasma and because it causes the particles to drift inward, increasing the plasma pressure. A higher pressure allows for easier examination of the behavior of the plasma (note that the pressure is still low enough that the plasma particles take minutes or hours to annihilate themselves). As a further application, the high pressure created in a dipole field opens up possibilities for nuclear fusion energy. See Ref. [1] for more information.

This paper is focused on the development of the levi-

tated dipole particle trap. The electromagnet that levitates the dipole is positioned above the vacuum chamber which houses the dipole and the plasma, and this configuration does not allow for stable levitation on its own. An analog control system is used to provide stability. The control system has been analyzed with the Laplace transform, showing that the system can be made stable (Ref. [2]). Here, a more exact model is produced, and the control system is numerically simulated to explore its behavior. Also, updated parameters are used, including parameters for the superconducting coil that will be used rather than for a permanent magnet.

The goals of this project have been to determine how to optimize the levitation control system (so that the superconducting coil levitates stably and does not oscillate), to explore the behavior of the control system, and to determine the system's response in certain worrisome situations.

II. MAGNETIC LEVITATION

The magnetic trap for the electron-positron plasma consists of a superconducting, floating (F) coil inside a vacuum chamber and a lifting (L) coil, with a programmable current source, on top of the vacuum chamber (see Fig. 1). The superconducting coil is charged with a current via induction before it is mechanically lifted into place. Then, the L coil is powered on so the mechanical lift can be lowered. As it turns out, the F coil can easily be given tilting stability just by the size and position of the L coil. However, only one of horizontal and vertical stability can be obtained this way. Horizontal motion is in two dimensions, so horizontal stability was chosen to be supplied by the design of the L coil. It is more practical to only need to control one dimension of motion, so vertical stability is left to be provided by other means.

See Ref. [2] for more detail about the magnetic levitation system.

A. Control System

Vertical stability of the F coil is maintained by an analog control system. The F coil's vertical position is monitored by laser rangefinders, and the average of their output signals serves as part of the input to a proportional-integral-differential (PID) control circuit. The output of the PID circuit controls the L coil's current source, changing the strength of the L coil's magnetic field. This in turn either raises or lowers the F coil toward its equilibrium position.

The "I" in PID refers to an integrator (gain proportional to the time integral of the input), which would create an equilibrium setpoint for the system to maintain. However, because of the nature and requirements of this levitation control system, no integrator is used, and the setpoint is instead indirectly provided by a reference voltage (V_{ref}): the full input to the PID circuit is the difference between this reference voltage and the averaged output of the laser rangefinders. The "P" and "D" in PID refer to a gain proportional to the input and a gain proportional to the time derivative of the input, respectively. With proper calibration of P, D, and V_{ref}, these two gains are sufficient to maintain a stable vertical position of the F coil.

V_{ref} is supplied by an external source, and it can be changed to alter the equilibrium position of the F coil. The proportional and differential gains in the PID circuit are implemented as operational amplifier components: the proportional gain is an inverting amplifier, and the differential gain is a practical differentiator ("practical" because there are an extra resistor and capacitor to filter out too-high and too-low frequencies). In both of these amplifier components, the resistor in the feedback position is variable, and varying these resistors changes the gains P and D. These resistances must be optimized both to ensure stability and to prevent the system from oscillating.

B. Time Response of System Components

Unlike idealizations, the components of this control system do not respond instantaneously to change. Instead, they all take different amounts of time to respond to a change before eventually steadying at a new state. See Fig. 2 for a visualization of the time response of an arbitrary system component.

Due to the natural delay before a system component responds completely to a change in its inputs, while the system is in a dynamic state, each component is really responding to the past states of previous components. This is important in the analysis of the control system because these time delays must be accounted for in order

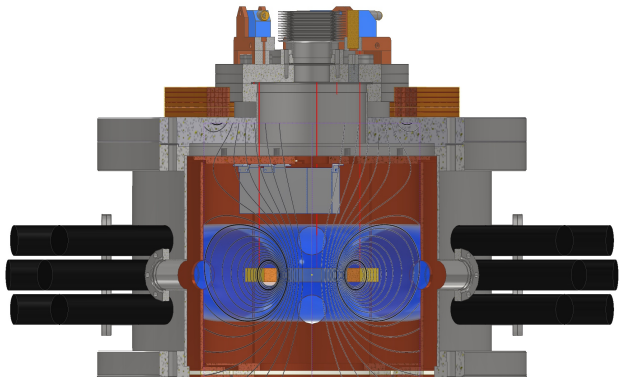

FIG. 1. The charged particle trap design. The superconducting F coil (yellow) floats inside the vacuum chamber. Positioned on top, the L coil (brown) lifts the F coil, and the laser rangefinders (blue) measure F coil height. Courtesy of Alexander Card (APEX).

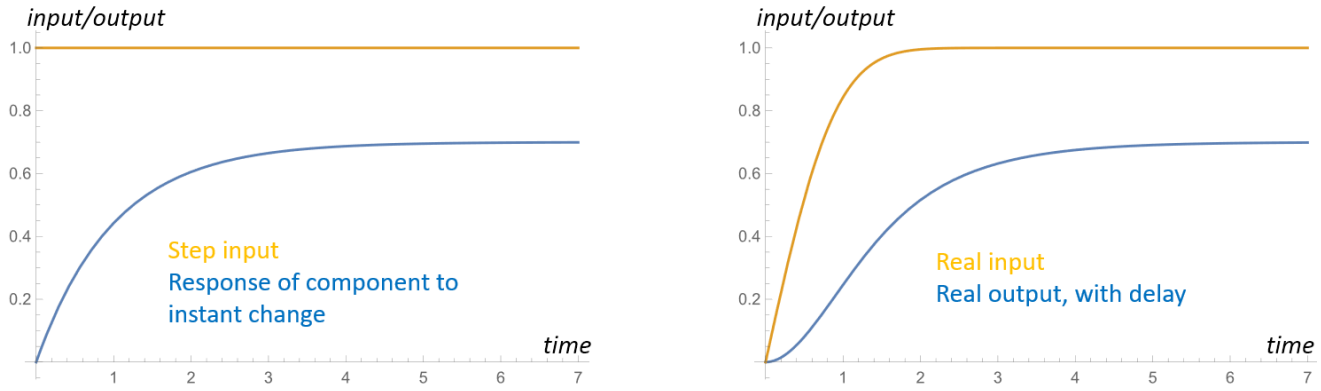

FIG. 2. The time response of an arbitrary control system component with gain 0.7. On the left is the exponential response to an instantaneous step in input. On the right is the response for a more realistic change in input.

to produce an accurate model. This can be accomplished with convolution, which is a binary, function operation. The output function is related to how one input responds to the other. For a visual example, examine Fig. 2. The blue output on the right is the convolution of (a) the orange input on the right and (b) the function describing the response of this arbitrary component (i.e., the blue output on the left flipped upside down so it decays to zero). The blue output on the right can be thought of as how the response of this arbitrary component is 'modified' by a non-instantaneous change in input. See Appendix A for a discussion on convolution.

The laser rangefinders respond very quickly to a change in the F coil position, so the effect of this delay on the system is small. The current source for the L coil has a slower response to changes in its input (still only a fraction of a second), so its delay has more significant effects on the system. Also, the magnetic field of the L coil induces eddy currents in the vacuum chamber walls. These eddy currents actually delay the effects of the magnetic field on the position of the F coil, so this is another time delay to account for. The eddy current time delays last about half as long as the current source time delays.

III. MODELING THE CONTROL SYSTEM

In Ref. [2], the control system is analyzed in the complex frequency domain with Laplace transform analysis. This method is convenient because it turns convolution, discussed in section II B and Appendix A, into multiplication. Also, it provides an easy way to test the system for stability. The system is stable if the real parts of the poles (roots of the denominator) of the system's Laplace-domain transfer function are negative. This corresponds to exponential decay, whereas positive real parts would correspond to exponential growth. To ensure that the poles have negative real parts, Ref. [2] uses the Routh-Hurwitz stability criterion.

Unfortunately, this analysis method has some drawbacks. First, the above requirement for the system transfer function's poles (checked with Routh-Hurwitz) only establishes stability. It does not determine anything about whether the system oscillates or not. This information is important because oscillation in the levitation system is undesirable. Second, it is difficult to perform Laplace transform analysis without approximations. When exact versions of the transfer functions are included for more of the system components, the denominator of the system's total transfer function becomes a higher-order polynomial (at least seventh-order). As the accuracy of the analysis increases, figuring out how to meet the requirement for the poles becomes increasingly challenging: it becomes difficult to directly find the poles, and the Routh-Hurwitz stability criterion becomes very computationally intensive.

In order to analyze the system accurately without these problems, numerical analysis methods are used here. The analysis is taken back into the time domain in order to easily visualize the behavior of the levitation control system. Using a numerical simulation allows for direct testing of stability and oscillation. The system can be simulated under specific conditions in order to test the effects of parameter values. However, in order to optimize parameters (such as P and D in the control circuit), the system must be simulated multiple times to compare different parameter values.

See Appendix B for more details about the following derivations.

A. Equation of Motion for F Coil

The point of interest of this analysis is the vertical position of the F coil. The purpose is to determine what ranges of parameters stabilize the vertical part of the F coil's levitation. For that reason, this analysis numerically solves a one-dimensional equation of motion for the F coil in order to understand the vertical part of its levitation in the time domain. The derivation of the equation of motion is based off of the same in Ref. [2].

Unlike the derivation in Ref. [2], the vertical (z) axis

is inverted here to match the direction of the laser rangefinders. Also, the origin is set to the center of the L coil instead of the equilibrium position of the F coil. This means that the variable z measures the distance below the center of the L coil (see Fig. 1 for a visual).

The F coil position is directly determined by the magnetic field of the L coil (aside from the effects of the eddy currents in the vacuum chamber walls, but those only add a time delay, not a change in the vertical response of the F coil). The vertical magnetic force on the F coil is proportional to the radial component of the L coil's magnetic field, at the radius of the F coil. The net vertical force on the F coil is

$$m_F \frac{d^2 z}{dt^2} = 2\pi r_F N_F I_F B_r + m_F g \tag{1}$$

where m_F is the mass of the F coil, r_F is its radius, N_F and I_F are the number of turns and the current per turn, B_r is the radial magnetic field (note that it is negative, pointing inwards), and g is the acceleration due to gravity.

In order to work with this equation, some changes need to be made. The radial magnetic field B_r is proportional to the L coil's current per turn I_L, so B_r can be expressed as $I_L h$ (where h is the rest of the expression for B_r, only related to geometry). Furthermore, I_L can be written as $I_{L0}\left(1+\frac{I_d}{I_{L0}}\right)$ with equilibrium current I_{L0} and perturbation from equilibrium over time I_d. Similarly, in order to account for changes in the F coil current, I_F is replaced by $\lambda_F I_{F0}$, where λ_F is a function of t that can be set manually to model possible F coil current fluctuations relative to the equilibrium current. Finally, h is replaced by $h_0\left(1+\frac{h_d}{h_0}\right)$, where h_d is a function of z. I_{L0} and h_0 are constants that must be calculated for each set of system parameters.

The new equation of motion is

$$\frac{d^2 z}{dt^2} = \frac{2\pi r_F N_F \lambda_F I_{F0}}{m_F} I_{L0}\left(1+\frac{I_d}{I_{L0}}\right) h_0 \left(1+\frac{h_d}{h_0}\right) + g. \tag{2}$$

This equation can be simplified by using equilibrium conditions to eliminate some constants. After further manipulation, the equation of motion simply becomes

$$\frac{d^2 z}{dt^2} = g - g\lambda_F(t)\left(\frac{I_L}{I_{L0}}\right)\left(\frac{h(z)}{h_0}\right). \tag{3}$$

h can be taken directly from the expression for B_r in Ref. [2], keeping in mind the reversed z direction. Thus, the only part still undetermined is I_L, which relates to the rest of the control system.

1. *Deriving $I_{L,eddy}$*

The quantity thus far referred to as $I_L(t)$ is the part of the control system that determines the motion of the F coil. To be more accurate, this is really the L coil current as experienced by the F coil. In other words, the quantity $I_L(t)$ in the section above is not the current in the L coil, but the L coil current taking into account the time delay caused by eddy currents. For the remainder of this paper, that quantity will be expressed as $I_{L,eddy}$, and I_L will refer to the actual L coil current.

In the control system, the laser rangefinders, the L coil current source, and eddy currents in the vacuum chamber walls all cause time delays. From Ref. [2], in the Laplace frequency domain, all three of these components can be closely approximated with first-order transfer functions in the following form:

$$\frac{output}{input} = G = \frac{\gamma}{1+s/\omega} \tag{4}$$

where γ is the gain of the component (with proper units), s is the complex frequency, and ω is the response frequency of the component, or the inverse of its time constant ($\omega = 1/\tau$).

In the time domain, after using an inverse Laplace transform, these transfer functions become

$$(output) = \gamma\omega e^{-\omega t} * (input) \tag{5}$$

where $*$ denotes convolution (see Appendix A). This general expression can be used to express quantities in the control system. For example, the L coil current as experienced by the F coil, $I_{L,eddy}$, is the output of the eddy current transfer function. Since the eddy currents only create a time delay, the gain γ is 1. The expression for $I_{L,eddy}$ in the time domain is then:

$$I_{L,eddy}(t) = \omega_{eddy} e^{-\omega_{eddy} t} * I_L(t). \tag{6}$$

A similar approach can be used for the rest of the control system. The L coil current is the output of the transfer function for the L coil current source. The input to that transfer function is the output of the PID circuit, which has its own transfer function. The input to the PID circuit is (recall) the difference between the externally-set reference voltage and the output of the laser rangefinders. Treating the three averaged laser rangefinders as a single one, the input to the laser rangefinder transfer function is in fact the vertical position of the F coil, plus an offset distance. So, in this way, $I_{L,eddy}$ depends on both t and z.

The transfer function of the PID circuit is necessary in order to build an expression for $I_{L,eddy}$. Since the integrator is not used, the transfer function is just the sum of the transfer functions for P and D. Assuming the proportional- and differential-gain amplifiers are ideal, the transfer function is

$$G_{\mathrm{PID}} = \mathrm{P} + \mathrm{D}s. \tag{7}$$

As mentioned before, the differentiator is not ideal. There are an extra resistor and an extra capacitor used to filter out noise, and these add a small time delay. For

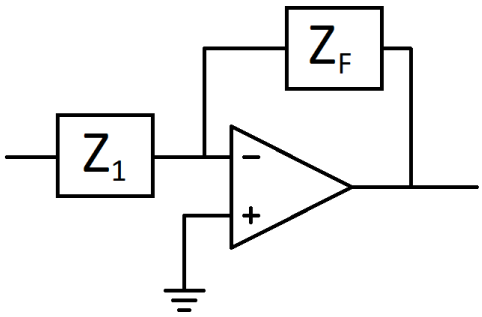

FIG. 3. The transfer function for this op amp component is $G = Z_F/Z_1$. This is the case for both the differentiator and the proportional gain amplifier, although this results in a complicated function for the differentiator while it gives a constant P.

greater accuracy, a more exact transfer function is used for the differentiator. The transfer function for an inverting operational amplifier component, which is the case here, is the ratio of the total impedance of the negative feedback loop of the amplifier, to the total impedance of the rest of the input to the minus terminal (see Fig. 3). The more exact transfer function replaces Ds above.

When all of this is put together to form an expression for $I_{L,eddy}$, there are multiple nested convolutions. Some of the convolutions that do not depend on z can be simplified. Afterwards, the expression is:

$$I_{L,eddy} = \gamma_2\gamma_5\omega_2\omega_3\omega_5 \left(\frac{e^{-\omega_2 t} - e^{-\omega_5 t}}{(\omega_2 - \omega_3)(\omega_2 - \omega_5)} + \frac{e^{-\omega_3 t} - e^{-\omega_5 t}}{(\omega_3 - \omega_2)(\omega_3 - \omega_5)} \right) * \Big(\mathrm{P}(z + z_{off}) + (z + z_{off}) * H(t) \Big) - \gamma_2 V_{ref} \mathrm{P} \tag{8}$$

Following Ref. [2], the subscripts 2, 3, and 5 refer to the L coil current source, the eddy current effects, and the laser rangefinders, respectively. $H(t)$ is the time-domain version of the differentiator's transfer function, and V_{ref} is the externally set reference voltage in the input to the PID circuit. Position offset z_{off} is included because the laser rangefinders do not measure from $z = 0$, at the center of the L coil. The last term is slightly approximated to reduce the amount of computation.

2. *Reference Voltage*

As mentioned earlier, the reference voltage V_{ref} in the PID circuit input creates a setpoint for the system. In other words, V_{ref} indirectly sets the equilibrium position for the F coil. Hence, V_{ref} must be set properly to ensure the F coil levitates at the desired vertical position.

At equilibrium, the L coil current must be equal to I_{L0}. This places a constraint on V_{ref}. In a steady state, the system has no time dependence, so time delays no longer have significance. Eq. 8 then becomes an expression for just I_L. The rest of the convolutions, beyond the eddy current effects, go away as well. This amounts to setting the complex frequency s to zero in all of the transfer functions and re-deriving Eq. 8. Set equal to equilibrium current I_{L0}, the result is the following equation:

$$I_{L0} = \gamma_2\gamma_5 P(z_{eq} + z_{off}) - \gamma_2 P V_{ref}, \tag{9}$$

where the equilibrium F coil position z_{eq} is used.

Solving this for V_{ref} gives

$$V_{ref} = \gamma_5(z_{eq} + z_{off}) - \frac{I_{L0}}{\gamma_2 P}. \tag{10}$$

This result is very useful for setting up the levitation control system and for deducing where the F coil will levitate for a given V_{ref} value.

IV. NUMERICALLY SOLVING THE EQUATION OF MOTION

Clearly, the vertical equation of motion for the F coil (Eq. 3) is not easily solved analytically. Numerical methods, coded in Python 3, are used to solve for the motion of the F coil under various conditions. The programs used can be found at Ref. [3].

Convolutions require integration over all time for each iteration of the differential equation solver. In order to have access to past values of position at a given time, a fourth-order Runge-Kutta algorithm is implemented rather than using a built-in differential equation solver.

A time step of less than about 10 µs was required to obtain unnoticeable errors. Compare this to a system response time to centimeter perturbations on the order of 0.1 s.

Both λ_F and V_{ref} are left as functions of t to allow freedom in creating control system scenarios to simulate. $h(z)$ is implemented as a rational approximation with a first-order numerator and second-order denominator in z. The approximation of h that is used is accurate to about 0.05% or less in the range of z tested.

The values of h_0 and I_{L0} need to be calculated for a given equilibrium z position and a given current-charge on the superconducting F coil. h_0 can be easily calculated from the rational approximation. An expression for I_{L0} follows from applying equilibrium conditions to Eq. 1:

$$I_{L0} = \frac{m_F g}{2\pi r_F N_F I_{F0}(-h_0)}. \tag{11}$$

The F coil starts at $t = 0$ with user-specified initial position and velocity. Time is extended to a few hundredths of a second before 0 in order to make convolutions consistent with reality (see Appendix A).

V. RESULTS OF SIMULATIONS

The virtual levitation control system was tested under various conditions in order to approximate how the physical apparatus should be expected to behave. The most important results are how parameters in the PID circuit, i.e., the values of P and D, affect the stability of the system. In addition to this, several scenarios were tested: electric noise in the control circuit, varying V_{ref} to adjust the F coil position, an oscillating I_F due to motion in a non-vertical dimension, and maxing out the L coil current source.

A. Effects of Changing Control Circuit Parameters

In the PID circuit, the values of the gains P and D are changed indirectly when certain variable resistors in the circuit are changed. Based on these resistors, the proportional gain P can range from 0.1 to 200.1. Since the differentiator is not ideal, describing its effects in terms of D is not completely accurate. However, in the tested range of differentiator gain, the difference in behavior from an ideal differentiator is small. Describing the differentiator's output as $\mathrm{D}(dV_{in}/dt)$ for input voltage V_{in} is a good approximation for making the differentiator easier to comprehend. So, keeping in mind that D does not describe the differentiator perfectly, D can range from about 0.001 to 1.88, with units of seconds.

The value of P needs to fall within a certain range in order to make the control system stable. This range is bounded below by about 0.9, which is determined by the steady-state gains of the control system components. The L coil current is mostly related to the amplification of P, especially when the F coil moves slowly. The L coil current must be high enough (indirectly, P must be high enough) to exert a magnetic force on the F coil that will overcome the force due to gravity.

The upper bound for P is determined by the value of D. It was found that for a given value of D, P must be below a certain value to make the system stable. Additionally, when P is too high in this stable range, the system oscillates as it responds to perturbations. P must then be lower than another, tighter bound in order for the system to be free of oscillation. See Fig. 4 for examples of the three general P ranges.

No bound was found on the value of D, besides the requirement that the value of D allows the existence of a stable P range. In general, a higher value of D creates a larger stable P range. For low values of D, a higher D also corresponds to a larger non-oscillating P range within the stable range. Interestingly, though, for D above a certain value, the system oscillates no matter what the value of P is.

Simulations show that, with all else the same, changing the value of P significantly changes the system response time (in the opposite direction). A large-scale example: for certain system parameters, including P set to 5, the F coil takes more than 0.6 seconds to move from a displacement of 5 mm back to equilibrium, but with similar parameters and P set to 70, the F coil only takes about 0.1 seconds to move the same distance. This example is not very applicable to the physical levitation system, for a P value of 70 is high enough that the system oscillates as it returns to equilibrium. On a more practical level, a reduction in P from 8 to 2 results in an increase in system response time from around 0.05 s to 0.1 s (with different parameters and now over a displacement of about 1.5 cm).

On the other hand, changing the value of D does not change the system response time by much. Raising D actually slightly increases the system response time, but this increase is balanced out by the larger range of stable P made available.

1. Optimizing P and D

It is desirable to know exactly what ranges of P and D cause the control system to respond optimally. That is, the system is stable, does not oscillate, and responds quickly to perturbation.

For a given value of D, the values of P are 'ordered' in how they affect the control system. Staying above the lower bound for P, increasing P always makes the system oscillate more, and decreasing P always makes the system oscillate less. This statement does not have much meaning in the low range of P for which the system simply does not oscillate. There, the ordering can be interpreted as: increasing P always brings the system closer to the oscillating range, and decreasing P always moves the system farther from that range.

Because of this ordering, the border between the oscillating and non-oscillating ranges of P values (for a given D) can be located with a binary search algorithm. The idea of this algorithm is as follows:

1. Begin with two P values, where the lower one is definitely in the non-oscillating range and the upper one is definitely in the oscillating range.

2. Find the midpoint of these two values (the arithmetic mean). Run a simulation using this midpoint

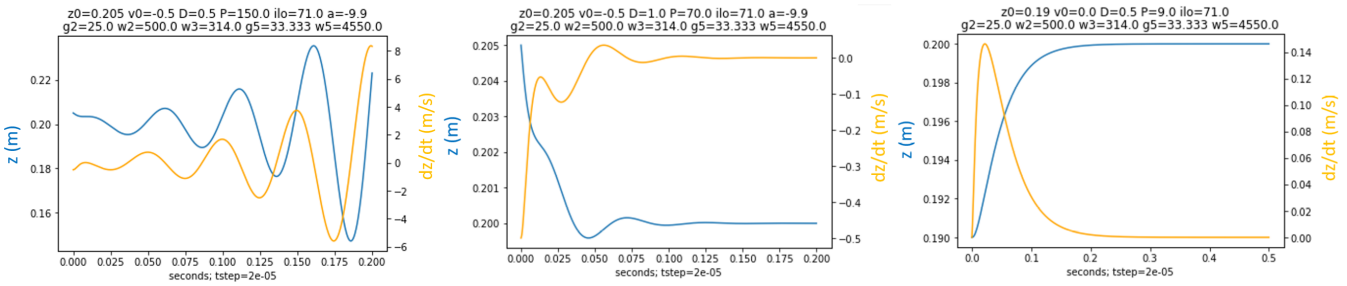

FIG. 4. Left to right: For a given value of D (the differential gain), P (the proportional gain) is (a) too high, and the system is unstable, (b) low enough that the system is stable, but high enough that it oscillates as it responds to displacement, and (c) low enough for the system to respond without oscillation. In each example, the F coil starts with some initial displacement and/or velocity. z is the distance below the center of the L coil. The text above each figure lists various parameters used for each simulation.

P value.

3. Test whether the resulting motion of the system oscillates.

   (a) If the system oscillates, the boundary between the two ranges is lower. Set the midpoint P value as the new upper P value.

   (b) Otherwise, the boundary is higher. Set the midpoint P value as the new lower P value.

4. Repeat from step 2 until the boundary is located to desired precision.

This process is implemented in order to find the boundary between the non-oscillating and oscillating ranges of P values for various D values. The results are shown in Fig. 5. The boundary was located for two different values of I_{L0}: 39 amps and 71 amps. These correspond to about 54000 amp-turns of current on the F coil and about 30000 amp-turns, respectively. It is clear that the non-oscillating P range is larger for higher D. The horizontal axis stops near the D value beyond which the system oscillates no matter the P value. This point is preceded by a leveling-off of the blue boundary.

Presumably, any point (D, P) underneath the boundary lines would make the system stable without oscillation, as desired, and moving farther to the right so that P can be higher would make the system respond faster. However, there is a singularity in the time-domain transfer function of the differentiator for a D value of about 0.4 s. (This corresponds to the variable resistor in the differentiator being set to approximately 42700 Ω, based on circuit component data provided in Ref. [2].) This D value should be avoided. Also, the system may not be completely free of oscillation when the variable resistor is higher than 50000 Ω (with a 54000 amp-turn F coil charge). For practicality, in the binary search algorithm, a simulation is tested for oscillation by determining whether the velocity of the F coil is monotonic. A more stringent test would be to check whether a higher derivative is monotonic. On the blue border beyond 50000 Ω, the system oscillates slightly despite having a monotonic velocity. In light of these concerns, the fastest safe system response time corresponds to D near 0.3 s and P in the upper part of its non-oscillating range.

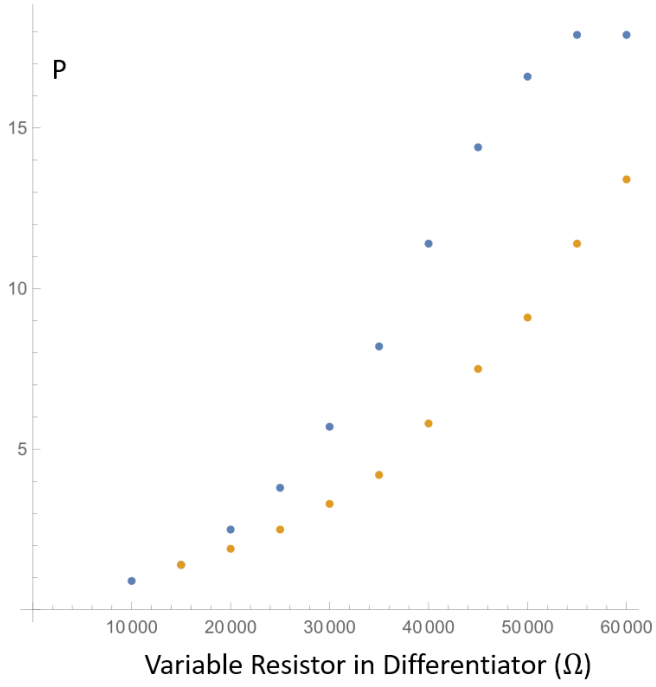

FIG. 5. The boundary between the ranges of P where the system oscillates (above the dots) and where the system does not oscillate (below the dots), located with a binary search algorithm. The blue boundary corresponds to an F coil current-charge of 54000 amp-turns, and the orange boundary corresponds to an F coil current-charge of 30000 amp-turns. The horizontal axis is in terms of the variable resistor in the differentiator that directly changes the differentiator's behavior (labeled R_{63} in Ref. [2]). The approximate differential gain D is equal to $R_{63} \cdot (9.4\ \mu\text{F})$.

B. Electric Noise in the Control System

Unwanted electric noise in the control system could be a cause for unexpected behavior in the magnetic levitation. Sources of noise could include random (white) background noise from the surrounding environment, power surges due to various events on a shared electrical grid, and line noise, which oscillates at the frequency of the AC power source or its harmonics.

Noise has a greater effect when it has a large voltage amplitude relative to the voltage of the system. Also, the differentiator could greatly amplify high-frequency noise because of its large derivative. In order to create greater effects, noise is inserted into the simulation at the input of the PID circuit, where the signal of the system is small and the noise can be amplified by the PID circuit. This is accomplished mathematically by adding the noise voltage to the reference voltage V_{ref}.

White noise, which generally has a very high frequency, is mostly filtered out by the filtering components of the differentiator. Hence, the very high derivative of the white noise is not amplified. However, if the white noise has a large enough amplitude relative to the PID input, the proportional gain amplifier can noticeably amplify the noise and cause some random motion in the F coil.

Simulating power surges shows that a surge changes the position of the F coil for some time. After the surge is done, the F coil returns to its original position. Inserting a power surge into the PID circuit input is equivalent to just changing the reference voltage for the duration of the surge (see section V C). For V_{ref} near 9 volts, which is a typical value, a change of 0.3 volts moves the F coil about a centimeter. However, the control system takes on the order of 0.1 seconds to respond to such a change, so if a power surge lasts less than 0.1 seconds, the F coil will not move that full distance before turning around back towards its equilibrium position. This fact allows, for instance, a 2 volt surge that lasts on the order of 1 ms to only move the F coil about 2 mm.

Unlike white noise, line noise in the lower harmonics of the power supply does not have a high enough frequency to be eliminated by the filters on the differentiator. Even so, the higher harmonics oscillate so much faster than the system can respond that there are only minor affects. The largest effects come from line noise oscillating at the first harmonic of the power supply (in Germany, AC power is supplied at 50 Hz). 50 Hz sinusoidal noise with an amplitude of 0.5 volts produces oscillations in the F coil position with amplitude less than half of a millimeter (at the same frequency as the noise).

See Fig. 6 for examples of the results of adding electric noise to the control system.

C. Varying the Reference Voltage

After the F coil is inductively charged with a current, it must be carefully raised to the position where it will trap plasma. There is a plan to raise the F coil part of the way with a mechanical lift, and then to raise it the rest of the way using the L coil. Instead of allowing the F coil to move upwards to its desired position very quickly, which could be risky, the equilibrium position can be set (via the reference voltage) to the position on the mechanical lift. Then, V_{ref} can be changed in order to move the F coil to its operating position.

Another reason for varying V_{ref} is to dynamically adjust the system as needed, for example when the F coil gradually loses current due to its small resistance.

Fig. 7 shows an example of the system's behavior when V_{ref} is changed gradually. The required change in V_{ref} for a particular desired change in equilibrium position is calculated with Eq. 10. As long as the change happens slower than the system responds, the F coil moves smoothly. Hence, varying the reference voltage is a viable way to adjust the F coil's vertical position.

D. F Coil Current Oscillation

This analysis of the levitation control system only examines the vertical motion of the F coil, ignoring any horizontal motion or tilting. A superconducting coil conserves magnetic flux passing through it, but it does not necessarily conserve current. If the F coil position oscillates in a horizontal direction between locations with different L coil magnetic field strengths, in order to conserve flux, the F coil current oscillates.

An oscillating F coil current is certainly a possibility, for the reason discussed above or other reasons. The effects of this on the vertical levitation control system are modeled by altering $\lambda_F(t)$, the function that describes relative changes in F coil current. The F coil current is assumed here to oscillate sinusoidally at a frequency of 2 Hz.

Because the control system responds on the order of 0.1 s, which is a bit smaller than the F coil oscillation period of 0.5 s, it is able to adjust to changes in position caused by I_F oscillations before they become very significant. Hence, for small amplitude I_F oscillations, the effects on the system are minor. For more extreme I_F oscillations, the vertical position of the F coil changes more noticeably. For example, when I_F oscillates with an amplitude that is half of I_{F0}, the F coil's position oscillates (at the same frequency) with an amplitude of about 2 mm.

E. Maxing Out L Coil Current Source

The L coil current source can supply between 0 and 250 amps to the L coil. This corresponds to the input that controls the current source ranging from 0 to 10 volts. If the input is out of this range, the L coil current will reach a cap and stop changing (until the input is back within the proper range). This should not affect the stability of

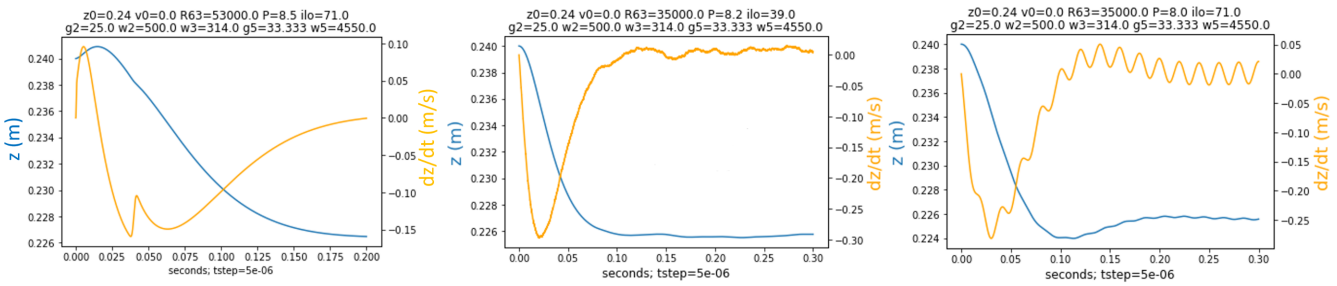

FIG. 6. The effects of three different types of noise on the levitation control system. On the left, a 0.5 V surge, lasting about 1 ms, causes the F coil to deviate from its path slightly. In the middle, 0.5 V maximum-amplitude white noise causes small, random motion in the F coil. On the right, 50 Hz sinusoidal line noise with amplitude 0.2 V causes the F coil's position to oscillate slightly. Note that in all cases, the motion of the blue line (position) is much more important to the functioning of the particle trap than the motion of the orange line (velocity).

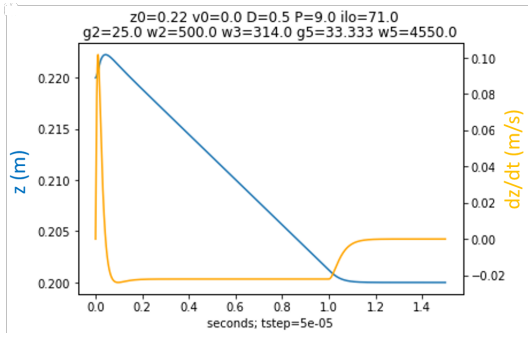

FIG. 7. V_{ref} is varied linearly over time, causing the F coil to move upwards (recall that z measures distance below the center of the L coil). Because V_{ref} is varied much slower than the system response time (on the order of 0.1 s), the F coil moves smoothly.

the control system. If the F coil drops down too low, the control system will make the L coil current stronger in order to raise the F coil back up. If the L coil current maxes out during this process, it will still raise the F coil. The F coil will just rise more slowly than if I_L had a larger range. The opposite case is similar.

It is useful to know when to expect the L coil current to reach its bounds. The L coil current is not directly calculated in the simulations described here, but an extra section of code is easily added to do so. Because the proportional gain P is generally larger than the differential gain D, and because the PID circuit input usually has a small derivative, the signal that controls the L coil current source is mainly influenced by P. Simulations find that, depending on the value of P, the equilibrium PID circuit output is around 1.5 or 2 volts. This means there is much more room for this signal to increase (it can go up to 10 V) than there is for it to decrease (it can go down to 0 V) before the L coil current reaches a bound. Even so, based on simulations, the F coil would have to be perturbed upward 5 or 6 mm to cause the PID output to reach 0 volts. From results discussed in section V B, moving the F coil this much would take a very large power surge.

VI. CONCLUSIONS

Numerical analysis provides a way to determine what the behavior of the levitation control system is like, given any system parameters, initial conditions, and changing system elements. This provides much more information than is possible for Laplace transform analysis. However, numerical simulations require a very small time step in order to be accurate, and the simulations take a lot of computation time, especially because multiple integrals over the entire simulation time must be performed at each time step. Most of the examples provided in this paper used around 50000 time steps, and the simulations for the optimization algorithm used around 80000. With a fourth-order Runge-Kutta scheme and two convolutions per equation of motion calculation, there are eight integrals performed for each time step.

Due to an instability in the differentiator and oscillations in the control system, the differential gain D should be kept below 0.4 s. The higher the proportional gain P is set, the faster the system will respond to perturbation, but P should be kept within the range shown in Fig. 5 in order to avoid oscillation. This range depends on how much current flows in the F coil.

There is a nice relationship between the reference voltage in the control circuit and the equilibrium position of the F coil (Eq. 10) which can be used to calculate either one from the other, given some additional parameters of the system. This relationship is useful for setting and maintaining an equilibrium levitation position. Also, the reference voltage can be safely varied to adjust this equilibrium position.

Overall, simulations of the magnetic levitation control system show promising stability, as long as the PID circuit is tuned properly. Electric noise does not pose an issue; high-frequency noise has very little effect, and slower noise must be very large to cause significant oscillations

in the F coil position. Similarly to low-frequency noise, oscillations in the F coil current do not affect the system much unless they have amplitude on the order of the F coil's own equilibrium current.

ACKNOWLEDGMENTS

I would like to acknowledge the help and guidance of Professors Jeffrey Collett (Lawrence University) and Matthew Stoneking (Lawrence University, APEX), and I would like to thank Professor Stoneking for offering me the opportunity to work with APEX. I would also like to acknowledge that Zachary Briscoe (Lawrence University, 2020) constructed a physical model of the levitation system discussed here, using a permanent magnet.

Appendix A: Convolution

Convolution, as used here, is defined as:

$$f(t) * g(t) \equiv \int_0^t f(t-\tau)g(\tau)d\tau. \tag{A1}$$

One function is flipped around and started at t, and then the product of the two functions is integrated within the bounds. The bounds on the integral are across the entire domain of the functions f and g, which in this case is from the beginning of the simulations ($t = 0$) to whatever time t the simulation happens to be at when the convolution is evaluated.

Convolution is commutative, associative, and distributive over addition. These properties are utilized when the expression for $I_{L,eddy}$ (Eq. 8) is simplified.

When a convolution is taken to the frequency domain by either a Laplace transform or a Fourier transform, it becomes a multiplication (and vice versa). The reverse fact,

$$\mathcal{L}^{-1}\{F(s) \cdot G(s)\} = f(t) * g(t), \tag{A2}$$

is useful in deriving the time-domain equation of motion for the F coil. In the frequency domain, the compounded effect of the various system components is represented by multiplying all of their transfer functions. When this is taken to the time domain, these multiplications between the transfer functions become convolutions of the time-domain transfer functions.

In simulations, using 0 as the lower bound for the convolution integrals causes problems. This is equivalent to starting the F coil at position 0 for all time before $t = 0$ and then instantaneously moving the F coil to its actual initial position at $t = 0$. The simulation responds accordingly, creating large spikes throughout the whole system that are not representative of the system's true behavior.

This is remedied by adding a 'history' for the convolutions. In the programs used, the positions of the F coil are stored in an array. A fraction of a second's worth of data is added before $t = 0$, where the F coil is kept stationary at its initial position. Time in the simulation is still started at zero, but this history is included in the convolution integrals. This way, the functions that are convolved with the F coil position are multiplied by the initial position before $t = 0$ rather than being abruptly cut off at zero. This creates a much smoother simulation that responds as though the F coil actually starts at its initial position instead of jumping there instantaneously.

Ideally, the 'history' for the convolutions would extend to $-\infty$. However, that is not feasible from a computation time standpoint. Also, the functions that are convolved with the F coil position decay exponentially, so it is really only important to include enough 'history' to cover the significant parts of these functions. This happens to be about 0.03 or 0.04 seconds.

In Python 3's scipy module, there is a function that performs convolution on discrete data structures. This was found to be faster than directly implementing the integral in the definition of convolution.

Appendix B: Details about Equation of Motion Derivation

The values of constants in the equation of motion were taken from APEX data.

Between Eq. 2 and Eq. 3, equilibrium conditions are used to eliminate some constants from the equation of motion. Those conditions are that the second derivative of z, the perturbation current I_d, and h_d are all zero, and that λ_F is 1. This gives:

$$0 = \frac{2\pi r_F N_F I_{F0}}{m_F} I_{L0} h_0 + g \tag{B1}$$

$$\frac{2\pi r_F N_F I_{F0}}{m_F} I_{L0} h_0 = -g. \tag{B2}$$

Substituting this into Eq. 2 gives:

$$\frac{d^2 z}{dt^2} = -g\lambda_F \left(1 + \frac{I_d}{I_{L0}}\right)\left(1 + \frac{h_d}{h_0}\right) + g. \tag{B3}$$

Using the definitions $I_L = I_{L0}(1+I_d/I_{L0})$ and $h = h_0(1+h_d/h_0)$ yields Eq. 3.

h, the radial component of the L coil magnetic field divided by the L coil current, is given in Ref. [2]. This function of position only depends on the geometry of the magnetic field. The exact expression is long and contains elliptic integrals, so a rational approximation was obtained:

$$h \approx -0.277 + \frac{0.11037 - 0.72138z}{0.04063 - 0.08349z + z^2}. \tag{B4}$$

This approximation is very accurate in the operating range of the F coil. From 0.2 m to 0.26 m below the center of the L coil, the error in h goes from -0.06% to $+0.04\%$, with zero error at $z = 0.226$ m (the planned equilibrium position of the F coil).

In the frequency domain, the equation of motion of the F coil is

$$Z(s) = \big[G_5(Z(s) + z_{off}) - V_{ref}\big] G_1 G_2 G_3 G_4 \qquad \text{(B5)}$$

where $Z(s)$ is the position of the F coil as a function of complex frequency, and all of the G_i are transfer functions:

- G_5 is the transfer function of the laser rangefinders (takes in F coil position plus offset, puts out a voltage signal)
- G_1 is the transfer function of the PID circuit (takes in the quantity in brackets, outputs a voltage signal to L coil current source)
- G_2 is the transfer function of the L coil current source (takes in voltage signal, puts out corresponding current in the L coil)
- G_3 is the transfer function of the eddy currents in the vacuum chamber wall (takes in L coil current, puts out L coil current as experienced by the F coil)
- G_4 is the transfer function that describes the F coil's motion in the L coil's magnetic field (takes in L coil current as experienced by the F coil, puts out F coil position).

Note that in Ref. [2], the input to the PID circuit is reversed so that the term in brackets above would be made negative. The planned location of the laser rangefinders has changed from below the F coil to above the F coil, necessitating an inversion of the PID circuit input.

The time-domain version of G_4 is given in Eq. 1. The frequency-domain equation above can be referenced in working through the derivation of $I_{L,eddy}$. Eq. 6 gives the time-domain version of G_3, and the discussion around Fig. 3 details the time-domain version of G_1. The final two are as follows:

$$I_L(t) = \gamma_2 \omega_2 e^{-\omega_2 t} * V_{out,PID}(t) \qquad \text{(B6)}$$

$$V_{out,laser} = \gamma_5 \omega_5 e^{-\omega_5 t} * (z(t) + z_{off}) \qquad \text{(B7)}$$

These can all be stitched together to find an expression for $I_{L,eddy}$, which has many nested convolutions. The properties of convolution described in Appendix A can be used to simplify this into an expression with only two nested convolutions.

As mentioned in section III A 1, the last term in the expression for $I_{L,eddy}$ is approximated in order to reduce unnecessary computation. The full term, after simplification and without the minus sign, is:

$$V_{ref}\gamma_2\omega_2\omega_3 \frac{e^{-\omega_2 t} - e^{\omega_3 t}}{\omega_3 - \omega_2} * \Big(\mathrm{P} + 1 * H(t)\Big). \qquad \text{(B8)}$$

This is similar to the constant that is written in Eq. 8, except this function starts at 0 at $t = 0$ and moves upward like $(1 - e^{-t})$, coming to an asymptote at $V_{ref}\gamma_2\mathrm{P}$. The exponential rise to this constant value is very fast and is almost negligible (it takes about 0.01 s). When the convolution 'history' is included (see Appendix A), this exponential rise becomes an artifact of the abrupt start at zero and is no longer important. Thus, it can be removed completely and replaced with the constant value in Eq. 8.

In the derivation of Eq. 10, the steady-state version of Eq. 8 is used. The frequency of a stationary system is 0, so the transfer functions given by Eq. 4 become:

$$G = \frac{\gamma}{1 + 0/\omega} = \gamma. \qquad \text{(B9)}$$

The inverse Laplace transform of a constant (to take this to the time domain) is the constant times a Dirac delta function:

$$\mathcal{L}^{-1}\{\gamma\} = \gamma\delta(t). \qquad \text{(B10)}$$

Conveniently, the convolution of a function with a Dirac delta function is just the function:

$$\gamma\delta(t) * f(t) = \gamma f(t). \qquad \text{(B11)}$$

In this way, the convolutions in Eq. 8 simply become multiplications with the steady-state gains of each system component.

[1] M. R. Stoneking *et al.* (APEX), A new frontier in laboratory physics: magnetized electron-positron plasmas, J. Plasma Phys. **86**, 155860601 (2020).

[2] H. Saitoh, M. R. Stoneking, and T. S. Pedersen (APEX), A levitated magnetic dipole configuration as a compact charged particle trap, Rev. Sci. Instrum. **91**, 043507 (2020).

[3] The code used for this project can be found at: github.com/acetocj/Simulation-of-Feedback-System-for-Magnetic-Levitation.